Formation of Cyanogen Chloride from the Reaction of Monochloramine with Formaldehyde

ERIK J. PEDERSEN III,[†]
EDWARD T. URBANSKY,[‡]
BENITO J. MARIÑAS,*,[§] AND
DALE W. MARGERUM*,[‡]

School of Civil Engineering and Department of Chemistry, Purdue University, West Lafayette, Indiana 47907, and Department of Civil and Environmental Engineering, University of Illinois, Urbana, Illinois 61801

Methanediol dehydrates to give formaldehyde, which reacts rapidly and reversibly with monochloramine to form *N*-chloroaminomethanol. Under drinking water conditions, *N*-chloroaminomethanol undergoes a relatively slow decomposition that eventually leads to the formation of cyanogen chloride (ClCN) in apparently stoichiometric amounts. The following reaction sequence is proposed: $CH_2(OH)_2 \leftrightarrows CH_2O + H_2O$; $CH_2O + NH_2Cl \leftrightarrows CH_2(OH)NHCl$; $CH_2(OH)NHCl \rightarrow CH_2NCl + H_2O$; $CH_2NCl \rightarrow HCl + HCN$; $CN^- + NH_2Cl + H^+ \rightarrow ClCN + NH_3$. These reactions were studied at 25.0 °C and an ionic strength of 0.10 M (NaClO$_4$). Stopped-flow photometry was used to monitor rapid, reversible reactions, and photometry was used to study relatively slow decomposition reactions. Equilibrium and rate constants for the addition of formaldehyde to monochloramine were $(6.6 \pm 1.5) \times 10^5$ M^{-1} and $(2.8 \pm 0.1) \times 10^4$ M^{-1} s^{-1}, respectively. The dehydration of *N*-chloroaminomethanol was catalyzed by both H$^+$ and OH$^-$, with respective rate constants of 277 ± 7 and 26.9 ± 5.6 M^{-1} s^{-1}. Under characteristic drinking water conditions, the decay of *N*-chloroaminomethanol is the rate-limiting step. *N*-Chloromethanimine, formed by the dehydration of *N*-chloroaminomethanol, had a decomposition rate constant of $(6.65 \pm 0.06) \times 10^{-4}$ s^{-1}. At the relatively high methanediol concentrations used in this study, the intermediary *N*-chlorodimethanolamine was formed by the rapid and reversible reaction of *N*-chloroaminomethanol with formaldehyde. *N*-Chlorodimethanolamine then decayed relatively slowly. The following reaction sequence is proposed: $CH_2(OH)NHCl + CH_2O \leftrightarrows \{CH_2(OH)\}_2NCl$; $\{CH_2(OH)\}_2NCl \rightarrow CH_2NCl + CH_2O + H_2O$. The equilibrium and rate constants for the addition of formaldehyde to *N*-chloroaminomethanol were $(9.5 \pm 2.5) \times 10^4$ M^{-1} and $(3.6 \pm 0.1) \times 10^3$ M^{-1} s^{-1}, respectively. The decomposition of *N*-chlorodimethanolamine was catalyzed by OH$^-$, with a rate constant of 19.2 ± 3.7 M^{-1} s^{-1}. *N*-Chlorodimethanolamine would not be present under typical drinking water treatment conditions.

* Corresponding author phone: (217)333-6961 (B.J.M.) or (765)-494-5268 (D.W.M); fax: (217)333-6968 (B.J.M.) or (765)494-0239 (D.W.M.); e-mail: marinas@uiuc.edu (B.J.M.) or margerum@chem.purdue.edu (D.W.M.).
† School of Civil Engineering, Purdue University.
‡ Department of Chemistry, Purdue University.
§ Department of Civil and Environmental Engineering, University of Illinois.

Introduction

Cyanogen chloride (ClCN) is a toxic disinfection byproduct (DBP) commonly observed in chloraminated drinking water (*1*). The formation of ClCN in natural waters and the corresponding role of water quality parameters are not well understood. This lack of information prompted the U.S. Environmental Protection Agency to include ClCN in the Information Collection Rule (ICR) (*2*). The ICR required quarterly monitoring of ClCN by public water systems using chloramines and serving populations of at least 100 000 with surface water or 50 000 with groundwater (*2*). The World Health Organization recently proposed a guideline value of 70 μg/L for all cyanide species (including cyanogen compounds) in drinking water (*3*).

Preliminary testing (*4, 5*) has shown that ClCN forms when monochloramine and formaldehyde are reacted at concentrations representative of drinking water treatment. Formaldehyde, also a common DBP, is formed during ozonation or chlorination of waters containing natural organic matter (*6–8*) and during through reaction of glycine with monochloramine (*9*). Monochloramine is commonly considered as a secondary disinfectant following ozonation.

In the present work, we show that formaldehyde reacts rapidly and reversibly with monochloramine to form *N*-chloroaminomethanol, $CH_2(OH)NHCl$, a carbinolamine or hemiaminal. This type of nucleophilic addition reaction is known to occur by attack of the lone electron pair of primary amines on the electrophilic carbonyl carbon of aldehydes (*10–15*). $CH_2(OH)NHCl$ decomposes relatively slowly to form *N*-chloromethanimine, $H_2C=NCl$, which can rapidly lose HCl to yield hydrocyanic acid. Cyanide ion and HCN are known to react rapidly with monochloramine to produce ClCN (*16*). In cases where monochloramine is present in excess of total formaldehyde (e.g., drinking water conditions), the conversion of formaldehyde to ClCN appears to be stoichiometric after accounting for ClCN decomposition by hydrolysis (*4, 5*). Although there are other possible formation pathways for ClCN in chloraminated drinking water (*17–20*), the reaction series from CH_2O to $CH_2(OH)NHCl$ to CH_2NCl to HCN to ClCN would appear to be a major pathway, particularly when pre-ozonation is employed.

To study the kinetics of the formation and subsequent decomposition of *N*-chloroaminomethanol, the concentration ratios of the reactants were varied from a slight excess of monochloramine to a large excess of formaldehyde. Under conditions of excess formaldehyde, a second rapid, reversible reaction of formaldehyde occurs with *N*-chloroaminomethanol to form *N*-chlorodimethanolamine, $\{CH_2(OH)\}_2NCl$, which also undergoes relatively slow decay. *N*-Chlorodimethanolamine would not be present at significant levels under drinking water treatment conditions. The formation and decomposition of this compound, however, affected reaction rates under experimental conditions used in this study and is therefore of interest. The major objectives of this investigation were to study the rapid formation reactions and also the relatively slow decay sequences of both *N*-chloroaminomethanol and *N*-chlorodimethanolamine.

Experimental Section

Reagents and Solutions. Formaldehyde solutions were prepared by dilution of a 37% stock solution also containing approximately 10% methanol. The stock solution was standardized gravimetrically by reacting with 5,5-dimethyl-1,3-cyclohexanedione and forming an insoluble adduct (*21*). Paraformaldehyde initially present in the stock solution was

allowed to depolymerize for several hours following dilution (*22*, *23*). Low concentrations of methanol (final concentrations of <0.25%) and trace levels of formic acid (a decomposition product of formaldehyde) (*24*) did not affect reaction rates or interfere with any of the reactants.

Monochloramine solutions were prepared by adding sodium hypochlorite solution dropwise to a rapidly stirred buffered solution of ammonium chloride until achieving a N/Cl molar ratio of 1.1. The pH of these stock solutions was adjusted to a value of 9 or greater in order to minimize disproportionation of monochloramine (*25*). Ammonium chloride solutions were prepared by dissolving the salt in water, and sodium hypochlorite solutions were prepared by dilution of a commercially available stock solution, which was standardized spectrophotometrically. Monochloramine solutions were also standardized spectrophotometrically prior to use (λ_{max} = 243 nm, ϵ_{243} = 461 M^{-1} cm^{-1}) (*36*).

Stock ClCN solutions were prepared gravimetrically by discharging a small amount of pressurized ClCN gas over a tared flask, which contained water acidified to a pH < 3 (to minimize ClCN hydrolysis). A small cylinder containing approximately 300 g of >99% pure ClCN (Solkatronic Chemicals, Inc., Fairfield, NJ) was used for this purpose. Once the weight stabilized, the flask was stoppered and the solution was mixed. Other stock solutions were prepared by dissolution of appropriate amounts of reagent-grade chemicals.

Instrumental Methods. A Durrum model 110 stopped-flow spectrophotometer interfaced to a computer with a MetraByte Dash-16 A/D converter was used to study rapid addition reactions. The absorbance was monitored at 242 nm. This wavelength gave optimum resolution for changes in absorbance during the conversion of reactants to products. All absorbance values were converted so that they corresponded to a 1 cm cell path length. The drive syringes as well as the observation cell were thermostated at 25.0 ± 0.1 °C. For a given set of conditions, 4−10 replicate tests were performed. Initial absorbance (A_0), equilibrium absorbance (A_e), and observed rate constant (k_{obs}) were estimated for each test by nonlinear least-squares fitting of absorbance data to rate expressions presented in the following section. Values reported for these parameters were the arithmetic average of each replicate set.

The rates of the slower decomposition reactions were studied by monitoring absorbances at 250 nm with a Perkin-Elmer Lambda 9 UV−Vis spectrophotometer interfaced to a computer. In most cases, absorbance measurements were recorded at this wavelength at a given time interval (time drive). Repetitive scans of a given wavelength range were also performed at a specified time interval to observe spectral changes. Reactions were initiated by two methods. For relatively slow reactions (e.g., p[H$^+$] 6−8, 25 °C), an aliquot of monochloramine was added to a rapidly stirred formaldehyde solution of equal volume. Under conditions where the reaction was expected to be faster, a T-mixer was used to provide rapid mixing of the reactants. The cell holder of the spectrophotometer was thermostated at 25.0 ± 0.1 °C for all experiments. The Teflon-stoppered quartz cells used were essentially gastight and headspace-free.

Membrane introduction mass spectrometry (MIMS) analyses were performed to provide evidence for the formation of the two proposed *N*-chloro species. The apparatus consisted of a Finnigan TSQ 700 mass spectrometer equipped with an alkylated silicone membrane in the probe. The sample was circulated through the membrane at a flow rate of 1.0 mL/min, and the probe temperature was either ambient or 66 °C. The intensity of ions with mass-to-charge ratio (*m/z*) in the range of 60−300 amu produced by electron impact ionization was recorded.

A Hewlett-Packard series II 5890 gas chromatograph (GC) equipped with a 5972 series mass selective (MS) detector was used to identify intermediates and products in methylene chloride extracts of reaction solutions. The temperature of a split/splitless injector was held at a constant value of 100 °C. A 60 m long Supelco VOCOL capillary column with 0.25 mm i.d. was used. The column oven was held at 35 °C for 6 min following injection, then increased at 2 °C/min to 70 °C, held constant for 30 s, increased at 20 °C/min to 120 °C, and held at that temperature for 5 min. The flow rate of the carrier gas, helium, was constant at 0.48 mL/min. The detector scanned for eluting compounds in the range of 10−300 amu.

A Varian 3300 GC equipped with a ^{63}Ni pulsed electron capture detector (ECD) was used in the analysis of ClCN in gas headspace samples. GC components included an on-column injector, and a 30 m long, 0.53 mm i.d. Supelco VOCOL fused silica capillary column. The temperatures of the injector, column, and detector were constant at 100, 35, and 290 °C, respectively. Nitrogen was used as carrier and makeup gas at respective flow rates of 6.1 and 26 mL/min.

An Orion model SA 720 digital pH meter equipped with a Corning combination electrode was used for pH measurements. The electrodes were calibrated so that the measured pH values could be converted to p[H$^+$] (p[H$^+$] = −log[H$^+$]). This was accomplished by monitoring the electrode response during a titration of standard NaOH with perchloric acid at an ionic strength of 0.1 M and then correlating pH measurements to the known p[H$^+$] values. For the slow decay reactions, measurements were generally taken immediately after the reaction started as well as in the middle of the reaction to confirm that the pH remained constant.

Gas Chromatography Sample Preparation. Headspace samples analyzed by GC-ECD were prepared by first filling a 17-mL vial approximately half-full with the solution of interest. The vial was sealed liquid-tight with Teflon tape, shaken vigorously for approximately 10 s, and allowed to equilibrate for 1−2 min. A 450-μL headspace gas sample was then captured with a gas-tight syringe equipped with gas-tight valve and injected into the GC-ECD.

Samples analyzed by GC−MS were prepared by first filling a 17-mL glass vial with screw cap and Teflon septa with 7 mL of the sample. One milliliter of methylene chloride was added to the vial and shaken vigorously for approximately 10 s. A 1.5 ± 0.1 μL methylene chloride sample was withdrawn with a syringe (after rapid equilibration) and injected into the GC−MS.

Experimental Matrix. A summary of experimental sets performed for this study is presented in Table 1. Experiments were designed to assess the role of p[H$^+$], initial formaldehyde concentration, buffer type, and buffer concentration in the kinetics of the initial formaldehyde addition reactions (sets AP-1−9) and decomposition kinetics of intermediaries (sets DP-1−7, DB-1−8, and DC-1).

Results and Discussion

Reaction Sequence. A sequence (eqs 1 and 2) analogous to that observed between formaldehyde and ammonia (*27*) is proposed for the reaction of formaldehyde with monochloramine:

$$CH_2O + NH_2Cl \underset{k_{-2}}{\overset{k_2}{\rightleftharpoons}} CH_2(OH)NHCl \qquad (1)$$

$$CH_2(OH)NHCl + CH_2O \underset{k_{-3}}{\overset{k_3}{\rightleftharpoons}} \{CH_2(OH)\}_2NCl \qquad (2)$$
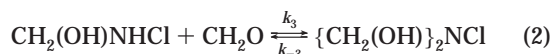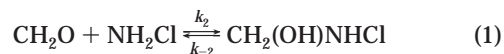
Both reactions are reversible and occur over a millisecond−second time scale for conditions used in this study. *N*-

exp set	p[H+]	[NH2Cl]0 (M)	[CH2O]T,0 (M)	type	buffer concn (M)
AP-1	6.95	0.000965	0.000486−0.00110	phosphate	0.015
AP-2	6.96	0.000957	0.000365−0.00142	phosphate	0.015
AP-3	6.96	0.000961	0.000243−0.00122	phosphate	0.015
AP-4[b]	7.34	0.00102	0.000779	phosphate	0.0140−0.0385
AP-5	6.69−7.73	0.00103	0.000768	phosphate	0.015
AP-6	6.70	0.00102	0.000771	phosphate	0.009−0.027
AP-7	6.89	0.000472	0.0512−0.273	phosphate	0.012
AP-8	6.91	0.000495	0.0338−0.203	phosphate	0.018
AP-9	7.19	0.000488	0.203	phosphate	0.0100−0.0225
DP-1	2.82−5.18	0.000493	0.0473	phosphate	0.020
DP-2	5.59−6.03	0.000488	0.0473	phosphate	0.020
DP-3	5.63−6.15	0.000483	0.0473	phosphate	0.020
DP-4	5.83−5.86	0.000488	0.0270−0.101	phosphate	0.020
DP-5	5.91−5.93	0.000494	0.0473	phosphate	0.014−0.035
DP-6	7.45−7.48	0.000491	0.0338	phosphate	0.011−0.021
DP-7	7.42−7.46	0.000491	0.101	phosphate	0.011−0.021
DB-1	8.36−8.65	0.000488	0.0473	borate	0.020
DB-2	8.64	0.000494	0.0270−0.101	borate	0.020
DB-3	9.05	0.000486	0.0203−0.101	borate	0.020
DB-4	8.17	0.000488	0.0270−0.101	borate	0.020
DB-5	8.89	0.000487	0.0338	borate	0.015−0.030
DB-6	8.88	0.000487	0.101	borate	0.015−0.030
DB-7	8.44	0.000497	0.0338	borate	0.012−0.030
DB-8	8.42	0.000497	0.101	borate	0.012−0.030
DC-1	9.23−10.23	0.000487	0.0473	carbonate	0.020

[a] Temperature = 25 °C, ionic strength = 0.1 M unless otherwise indicated. [b] Ionic strength = 0.2 M to allow for a broader total buffer concentration range.

Chloroaminomethanol and *N*-chlorodimethanolamine then decay relatively slowly to form *N*-chloromethanimine (eqs 3 and 4) as previously reported (*28, 29*):

$$CH_2(OH)NHCl \xrightarrow{k_4} CH_2NCl + H_2O \quad (3)$$

$$\{CH_2(OH)\}_2NCl \xrightarrow{k_5} CH_2O + CH_2NCl + H_2O \quad (4)$$
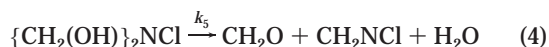
N-Chloromethanimine decomposes to hydrogen cyanide (*28, 30*) and hydrogen chloride:

$$CH_2NCl \xrightarrow{k_6} HCN + HCl \quad (5)$$

The hydrogen cyanide dissociates and reaches equilibrium with cyanide ion:

$$HCN \xrightleftharpoons{K_a} CN^- + H^+ \quad (6)$$

with $pK_a = 9.01$ at 25 °C and $\mu = 0.1$ M (*31*). Finally, cyanide ion reacts with monochloramine to form cyanogen chloride and ammonia via the general acid-catalyzed reaction (*16*):

$$CN^- + NH_2Cl + H^+ \xrightarrow{k_7} ClCN + NH_3 \quad (7)$$
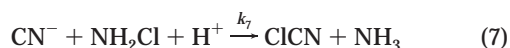
with a rate constant of 4.32×10^{10} M^{-2} s^{-1} at $\mu = 1.0$ M (NaClO$_4$) and 25 °C (*16*).

Formaldehyde forms a stable *gem*-diol, methanediol, in aqueous solution:

$$CH_2(OH)_2 \xrightleftharpoons[k_{-1}]{k_1} CH_2O + H_2O \quad (8)$$
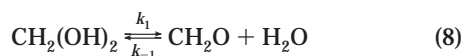
The equilibrium in eq 8 is shifted almost entirely to the left, i.e., most of the total formaldehyde present in the form of methanediol in dilute aqueous solutions (*24*). The dehydration reaction undergoes general acid−base catalysis; rate constants for H$^+$, H$_2$O, H$_2$PO$_4^-$, HPO$_4^{2-}$, and OH$^-$ were 2.7

M^{-1} s^{-1}, 5.1×10^{-3} s^{-1}, 0.088 M^{-1} s^{-1}, 0.39 M^{-1} s^{-1}, and 1600 M^{-1} s^{-1}, respectively, at 25 °C and an ionic strength (μ) of 0.2 M (*32*). The equilibrium constant for eq 8 at 25 °C in the presence of phosphate is (*33*)

$$K_1 = \frac{[CH_2O]}{[CH_2(OH)_2]} = 6.31 \times 10^{-4} + 5.1 \times 10^{-4}[H_2PO_4^-] + 21.6 \times 10^{-4}[HPO_4^{2-}] \quad (9)$$

Formaldehyde also tends to polymerize at relatively high concentrations. The predominant polymeric species at the highest concentrations investigated in this study ([CH$_2$O]$_T$ = 0.27 M) were the dimer and trimer, which form according to

$$2HO(CH_2O)H \xrightleftharpoons{K_{di}} HO(CH_2O)_2H + H_2O \quad (10)$$

$$HO(CH_2O)_2H + HO(CH_2O)H \xrightleftharpoons{K_{tri}} HO(CH_2O)_3H + H_2O \quad (11)$$
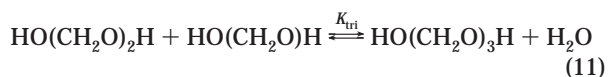
K_{di} and K_{tri} have reported values of 0.083 and 0.12 M^{-1}, respectively (*34*). Methanediol concentrations were calculated after taking eqs 10 and 11 into consideration for all cases in which polymer formation was appreciable ([CH$_2$O]$_T \geq 40$ mM).

UV Spectral Evidence for *N*-Chloroaminomethanol and *N*-Chlorodimethanolamine. For the rapid and reversible formaldehyde addition reactions (eqs 1 and 2), there are three species of interest that absorb in the UV region: NH$_2$Cl, CH$_2$-(OH)NHCl, and {CH$_2$(OH)}$_2$NCl. These molecules absorb due to $n-\pi^*$ electronic transition at the N−Cl bond. Formaldehyde, methanediol, and their polymeric species do not absorb in this region. Figure 1 presents equilibrium spectra corresponding to several solutions prepared with initial total formaldehyde concentrations in the range of 0−0.11 M and a constant initial monochloramine concentration of 0.457 mM. All solutions were buffered with phosphate at a total
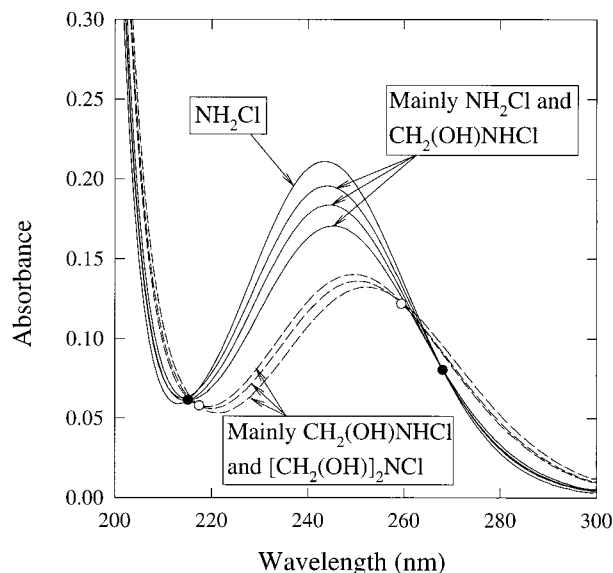
FIGURE 1. Equilibrium spectra of solutions resulting from the reaction of 0.457 mM monochloramine with formaldehyde at initial concentrations ranging from 0 to 0.114 M. Additional experimental conditions: $p[H^+] = 7.84 \pm 0.10$, $[PO_4]_T = 0.010$ M, 25.0 ± 0.1 °C, $\mu = 0.1$ M (NaClO$_4$), reaction time = 3–5 min.

concentration $[PO_4]_T \approx [H_2PO_4^-] + [HPO_4^{2-}]) = 0.01$ M, $p[H^+] = 7.84 \pm 0.10$, $\mu = 0.10$ M, and 25.0 ± 0.1 °C. The curves corresponding to relatively low methanediol concentrations (0–4.5 mM) had isosbestic points (filled circles in Figure 1) consistent with an equilibrium between two absorbing compounds, proposed to be NH$_2$Cl and CH$_2$(OH)NHCl. The spectra of solutions with greater total formaldehyde concentrations deviated from these isosbestic points, indicating the presence of at least a third absorbing species; this is proposed to be {CH$_2$(OH)}$_2$NCl. New isosbestic points were reached (open circles in Figure 1) at methanediol concentrations of 32–110 mM, consistent with an equilibrium between CH$_2$(OH)NHCl and {CH$_2$(OH)}$_2$NCl. The spectral shift presented in Figure 1 was similar to that reported for the NH$_2$Cl–CH$_3$NHCl–(CH$_3$)$_2$NCl system (*35*).

Mass Spectral Evidence of Intermediates and Products. A monochloramine solution, prepared by adding 7.5 mM hypochlorite to 12.5 mM ammonium chloride, was reacted with 100 mM total formaldehyde. The reaction solution was analyzed by MIMS within 2 h. Strong signals for ions with m/z values of 82 and 84 amu at the expected isotopic ratio for chlorine revealed the presence of CH$_2$(OH)NHCl. This experiment also provided evidence for the existence of {CH$_2$(OH)}$_2$NCl, with weaker signals at 111 and approximately 113.

Another test was performed by reacting 123 mM total formaldehyde with 20.4 mM monochloramine at pH 8. Methylene chloride extracts were analyzed by GC–MS after elapsed times of 8, 127, 229, and 331 min. *N*-Chloromethanimine was identified as a rapidly forming intermediate, which decayed slowly and was not present at significant levels by the end of the test. ClCN was also identified; the increase in its concentration corresponded qualitatively to the loss of *N*-chloromethanimine. The observation of significant amounts of *N*-chloromethanimine was somewhat unexpected; at pH 8, this species should not accumulate to appreciable levels in the reaction solution. A possible explanation for its presence is that *N*-chloroaminomethanol undergoes thermally induced dehydration inside the GC–MS injection port (100 °C). Another possibility is that *N*-chloroaminomethanol dehydrates in methylene chloride.

Identification of ClCN by GC-ECD. The formation of ClCN was also confirmed in an experiment at $p[H^+]$ of 5.6.
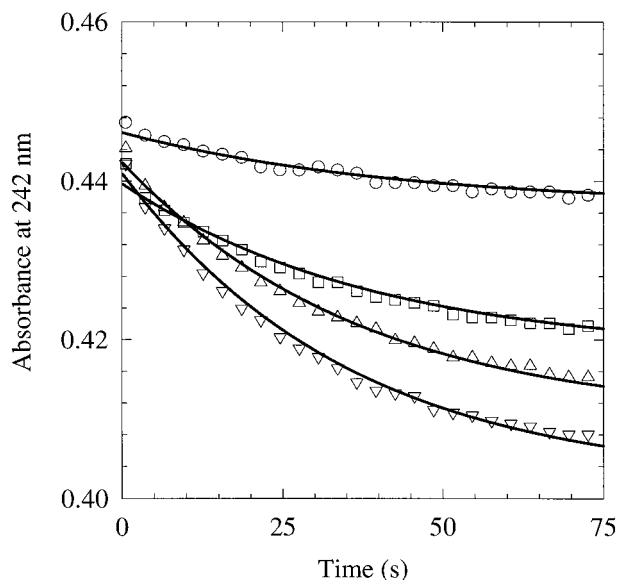
FIGURE 2. Experimental and predicted stopped-flow traces resulting from the reaction between monochloramine ($[NH_2Cl]_0 = 0.961 \pm 0.004$ mM) and formaldehyde ($[CH_2O]_{T,0} = (\bigcirc)$ 0.243, ($\square$) 0.608, ($\triangle$) 0.972, and ($\triangledown$) 1.22 mM). Additional experimental conditions: $p[H^+] = 6.96 \pm 0.03$, $[PO_4]_T = 0.015$ M, 25.0 ± 0.1 °C, $\mu = 0.1$ M (NaClO$_4$) (set AP-3, Table 1).

Additional conditions included $[NH_2Cl]_0 = 0.492$ mM, $[CH_2O]_{T,0} = 47.3$ mM, and $[PO_4]_T = 49$ mM. Headspace GC-ECD analysis revealed the presence of a large peak at an elution time identical to that of ClCN.

Reaction between Formaldehyde and Monochloramine. The reaction of formaldehyde with monochloramine (eq 1) was relatively fast. Kinetic analysis was complicated somewhat by the subsequent reaction of formaldehyde with *N*-chloroaminomethanol (eq 2), which was also rapid though somewhat slower. This interference was minimized by performing stopped-flow experiments at relatively low $[CH_2O]_{T,0}$; concentrations ranged from 0.243 to 1.42 mM (sets AP-1–3, Table 1). Representative results obtained for experimental set AP-3 are presented in Figure 2 in terms of decreasing absorbance at 242 nm with increasing reaction time.

The low reactant dosages used to isolate eq 1 resulted in relatively small changes in species distribution and absorbance. Kinetic data obtained under these conditions can be analyzed by the chemical relaxation, or concentration jump, method (*36*). The kinetic system is given by

$$A \underset{k_{-1}}{\overset{k_1}{\rightleftharpoons}} B + H_2O \tag{12}$$

$$B + C \underset{k_{-2}}{\overset{k_2}{\rightleftharpoons}} D \tag{13}$$

where A = CH$_2$(OH)$_2$, B = CH$_2$O, C = NH$_2$Cl, and D = CH$_2$(OH)NHCl. Corresponding changes in concentrations of the species involved are

$$\frac{d\delta_A}{dt} = -k_1\delta_A + k_{-1}\delta_B \tag{14}$$

$$\frac{d\delta_B}{dt} = k_1\delta_A - (k_{-1} + k_2[C]_e)\delta_B - k_2[B]_e\delta_c + k_{-2}\delta_D \tag{15}$$

$$\frac{d\delta_c}{dt} = \frac{-d\delta_D}{dt} = -k_2[C]_e\delta_B - k_2[B]_e\delta_C + k_{-2}\delta_D \tag{16}$$

where the subscript e denotes equilibrium, and δ is the

TABLE 2. Summary of Rate and Equilibrium Constants Determined for the Reactions of Formaldehyde with Monochloramine and N-Chloroaminomethanol, the Decomposition Reactions of N-Chloroaminomethanol, N-Chlorodimethanolamine, and N-Chloromethanimine, and the Equilibrium Constant for Cyclic Borate Ester Formation[a]

reaction	constant
$CH_2O + NH_2Cl \rightleftharpoons CH_2(OH)NHCl$	$k_2^0 = (2.8 \pm 0.1) \times 10^4 \ M^{-1}\,s^{-1}$
	$k_2^{HPO_4} = (7.5 \pm 0.6) \times 10^5 \ M^{-2}\,s^{-1}$
	$K_2 = (6.6 \pm 1.5) \times 10^5 \ M^{-1}$
$CH_2O + CH_2(OH)NHCl \rightleftharpoons \{CH_2(OH)\}_2NCl$	$k_3^0 = (3.6 \pm 0.1) \times 10^3 \ M^{-1}\,s^{-1}$
	$k_3^{HPO_4} = (8.2 \pm 0.7) \times 10^4 \ M^{-2}\,s^{-1}$
	$K_3 = (9.5 \pm 2.5) \times 10^4 \ M^{-1}$
$CH_2(OH)NHCl \rightarrow CH_2NCl + H_2O$	$k_4^H = 277 \pm 7 \ M^{-1}\,s^{-1}$
	$k_4^{OH} = 26.9 \pm 5.6 \ M^{-1}\,s^{-1}$
$\{CH_2(OH)\}_2NCl \rightarrow CH_2O + CH_2NCl + H_2O$	$k_5^{OH} = 19.2 \pm 3.7 \ M^{-1}\,s^{-1}$
$CH_2NCl \rightarrow HCN + HCl$	$k_6^0 = (6.60 \pm 0.20) \times 10^{-4} \ s^{-1}$
	$k_6^{OH} = (1.47 \pm 0.19) \times 10^6 \ M^{-1}\,s^{-1}$
$B(OH)_3 + \{CH_2(OH)\}_2NCl \rightleftharpoons ClN(CH_2O)_2B(OH)_2^- + H_2O + H^+$	$K_B = (1.42 \pm 0.46) \times 10^{-7}$

[a] Conditions: $\mu = 0.10$ M (NaClO$_4$), 25 °C.

difference between equilibrium and actual concentrations (e.g., $\delta_A = ([A]_e - [A])$). Equations 15 and 16 were obtained after neglecting a relatively small nonlinear term with the form $k_2\delta_B\delta_C$. Under the experimental conditions used, B can be regarded as a low-level, steady-state species (36). The steady-state concentration jump ($\delta_{B,ss}$) can be estimated by setting eq 15 equal to zero:

$$\delta_{B,ss} = \frac{k_1\delta_A - k_2[B]_e\delta_C + k_{-2}\delta_D}{k_{-1} + k_2[C]_e} \quad (17)$$

Substitution of eq 17 and mass balance conditions $\delta_B = -\delta_A - \delta_D$ and $\delta_C = -\delta_D$ into eq 16 gives

$$\frac{d\delta_D}{dt} = -\left(\frac{(k_1 - k_2[B]_e - k_{-2})}{k_1 + k_{-1} + k_2[C]_e}k_2[C]_e + k_2[B]_e + k_{-2}\right)\delta_D = -k_{obs}\delta_D \quad (18)$$

where k_{obs} is the observed first-order relaxation rate constant, and $[C]_e$ and $[B]_e$ are

$$[C]_e = \frac{1}{2}\left([C]_0 - [A]_0 - \frac{k_{-1}k_{-2}}{k_1k_2} + \sqrt{\left([C]_0 - [A]_0 - \frac{k_{-1}k_{-2}}{k_1k_2}\right)^2 + 4\frac{k_{-1}k_{-2}}{k_1k_2}[C]_0}\right) \quad (19)$$

$$[B]_e = \frac{k_1}{k_{-1}}([A]_0 - [C]_0 + [C]_e) \quad (20)$$

Observed absorbances, A, can be related to δ_D with

$$(A - A_e) = l(\epsilon_C - \epsilon_D)\delta_D \quad (21)$$

where A_e is the equilibrium absorbance, ϵ_C and ϵ_D are the molar absorptivities for C and D, respectively, and l is the light pathway length in the spectrophotometer cell. Equation 21 can be used to substitute δ_D for $(A - A_e)$ in eq 18, and the resulting equation can be integrated to obtain

$$(A - A_e) = (A_0 - A_e)e^{-k_{obs}t} \quad (22)$$

where A_0 is the initial absorbance.

Values of k_{obs}, A_0, and A_e were determined by fitting experimental absorbance data to eq 22 by nonlinear least-squares regression. Resulting average k_{obs} values were plotted in Figure 3 against corresponding initial methanediol concentrations. Rate constants k_2 and k_{-2} were then obtained by fitting k_{obs} values to the expression inside the parenthesis of eq 18. Resulting values for k_2 and k_{-2} and corresponding
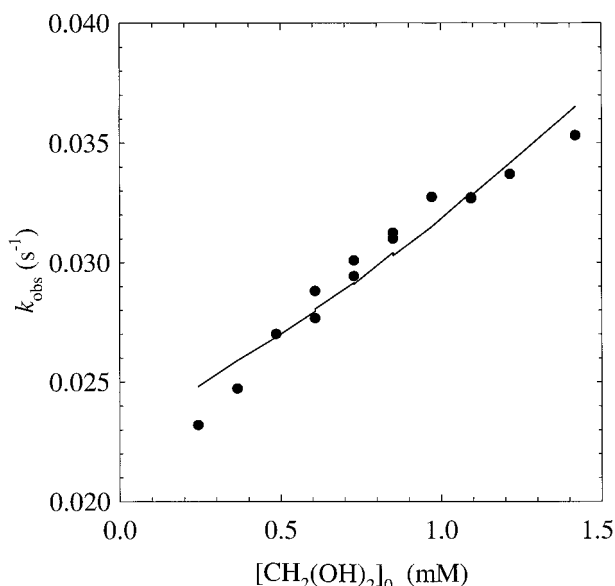
FIGURE 3. Observed and fitted apparent first-order rate constants corresponding to relaxation experiments as a function of [CH$_2$(OH)$_2$]$_0$. Experimental conditions: [CH$_2$O]$_{T,0}$ = 0.243–1.42 mM, [NH$_2$Cl]$_0$ = 0.961 ± 0.004 mM, p[H$^+$] = 6.96 ± 0.03, [PO$_4$]$_T$ = 0.015 M, 25.0 ± 0.1 °C, μ = 0.1 M (NaClO$_4$) (sets AP-1–3, Table 1).

TABLE 3. Molar Absorptivities of Relevant Compounds

species	wavelength (nm)	ϵ (M^{-1} cm^{-1})
NH$_2$Cl	242	459
	250	429
CH$_2$(OH)NHCl	242	326 ± 7
	250	345 ± 14
{CH$_2$(OH)}$_2$NCl	242	226 ± 15
	250	280 ± 5
CH$_2$NCl	250	186 ± 1
ClN(CH$_2$O)$_2$B(OH)$_2^-$	250	313 ± 2

equilibrium constant, $K_2 = k_2/k_{-2}$, are presented in Table 2. The average K_2 value, the equilibrium absorbance A_e of each trace, and the molar absorptivity for monochloramine (Table 3) were used to obtain the molar absorptivity for N-chloroaminomethanol at the experimental wavelength of 242 nm (Table 3).

The occurrence of general base catalysis was assessed by performing experiments at [PO$_4$]$_T$ = 9–38.5 mM and p[H$^+$] = 6.69–7.73 (sets AP-4–6, Table 1). Equilibrium constants used for H$_2$PO$_4^-$ and H$_2$O were pK_a = 6.72 and pK_w = 13.78 both at 25 °C and μ = 0.1 M (31). The relatively narrow p[H$^+$]
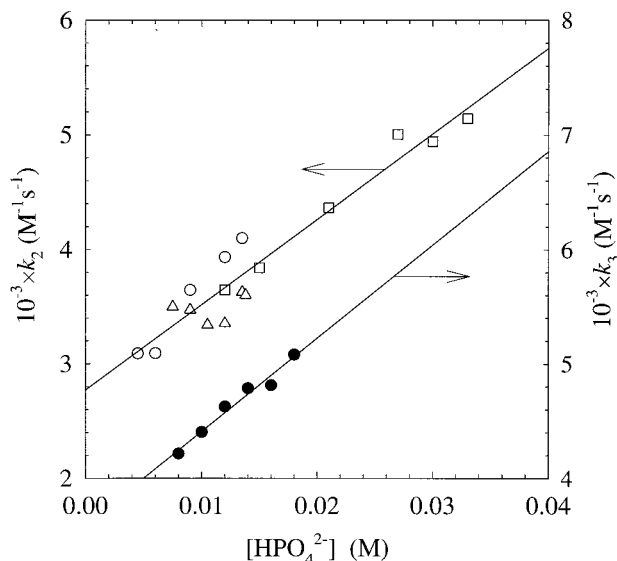
FIGURE 4. Effect of HPO_4^{2-} concentration on k_2 for experimental sets performed at ($\bigcirc$) $p[H^+] = 6.70 \pm 0.01$, $[PO_4]_T = 0.009-0.027$ M, $\mu = 0.1$ M; ($\square$) $p[H^+] = 7.34 \pm 0.02$, $[PO_4]_T = 0.0140-0.0385$ M, $\mu = 0.2$ M; ($\triangle$) $p[H^+] = 6.69-7.73$, $[PO_4]_T = 0.015$ M, $\mu = 0.1$ M (sets AP-4-6, Table 1) and k_3 for an experimental set performed at ($\bullet$) $p[H^+] = 7.19 \pm 0.04$, $[PO_4]_T = 0.0100-0.0225$ M, $\mu = 0.1$ M (NaClO$_4$); $[CH_2O]_{T,0} = 0.203$ M, $[NH_2Cl]_0 = 0.488 \pm 0.020$ mM, 25.0 ± 0.1 °C (set AP-9, Table 1).

range and low buffer concentrations were selected to minimize the acid—base-catalyzed decomposition of N-chloroaminomethanol, a reaction discussed subsequently. Equation 22 was used to analyze the data for each trace, with $k_{-2} = k_2/K_2$ and K_2 equal to the average value determined from the relaxation experiments (Table 2). Data analysis revealed that HPO_4^{2-} was the only base with an appreciable catalytic effect under the conditions investigated. The buffer dependence of k_2 (see Figure 4) could therefore be represented with

$$k_2 = k_2^0 + k_2^{HPO_4}[HPO_4^{2-}] \tag{23}$$

Base catalysis constants estimated by linear regression of the k_2 data shown in Figure 4 are presented in Table 2. The reverse rate constants, k_{-2}^0 and $k_{-2}^{HPO_4}$, can be calculated by dividing the respective forward rate constants by K_2. Within the relatively narrow $p[H^+]$ range and at the reaction times studied, the slow, acid—base-catalyzed decomposition of N-chloroaminomethanol did not interfere with the determination of k_2 and k_{-2}.

The equilibrium and rate constants presented in Table 2 for eq 1 were used to predict all absorbance traces performed at relatively low total formaldehyde concentrations. As illustrated in Figure 2, good agreement was generally observed between experimental and predicted traces.

Reaction between Formaldehyde and N-Chloroaminomethanol. The reaction of formaldehyde with N-chloroaminomethanol (eq 2) was analyzed by performing tests with methanediol in large excess compared to monochloramine. Under these conditions and after N-chloroaminomethanol reached peak concentration, eqs 1 and 8 can be assumed to be in rapid preequilibrium as compared to eq 2. The system could thus be represented with eqs 12 and 13 at preequilibrium as

$$B + D \underset{k_{-3}}{\overset{k_3}{\rightleftarrows}} \rightleftharpoons E \tag{24}$$

with B = CH$_2$O, D = CH$_2$(OH)NHCl, and E = {CH$_2$(OH)}$_2$-NCl.
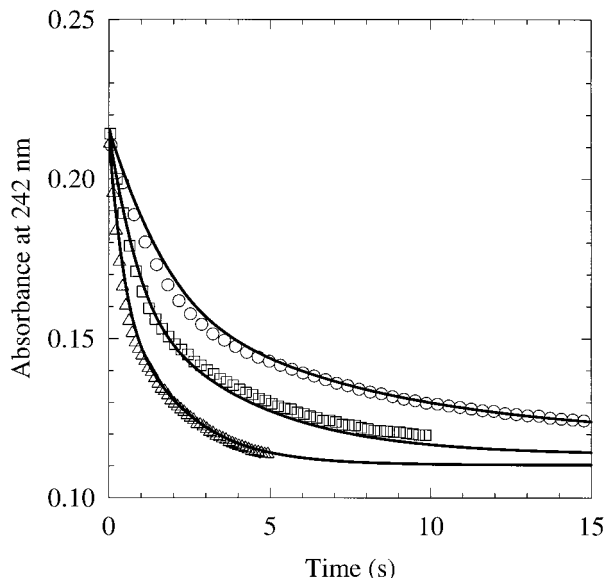
FIGURE 5. Experimental and predicted stopped-flow traces resulting from the reaction between monochloramine ($[NH_2Cl]_0 = 0.472$ mM) and formaldehyde ($[CH_2(OH)_2]_0 = $ ($\bigcirc$) 50.8, ($\square$) 100, and ($\triangle$) 198 mM) (set AP-7, Table 1).

The effect of methanediol concentration on k_3 under these pseudo-first-order conditions was investigated with experimental sets AP-7 and AP-8 (Table 1). Typical traces obtained are presented in Figure 5. Changes in absorbance were monitored for overall reaction times of at least three times that required for preequilibration of eq 1 (i.e., nearly complete disappearance of monochloramine). Data corresponding to reaction times after preequilibration of eq 1, or after the first one-third of the overall duration of each experiment, could be represented with

$$\frac{d\delta_D}{dt} = \frac{-d\delta_E}{dt} = -(k_3[B]_0 + k_{-3})\delta_D = -k_{obs}\delta_D \tag{25}$$

where $[B]_0$ is the constant concentration of formaldehyde, and k_{obs} is the apparent first-order rate constant. Equation 25 could now be converted to an expression with the form of eq 22. Average k_{obs} values, obtained by nonlinear least-squares regression, are presented in Figure 6 as a function of corresponding methanediol concentration. The linear dependence of k_{obs} on $[CH_2(OH)_2]_0$ for each set was consistent with eq 25. Differences between the two lines revealed that base catalysis was affecting the kinetics of eq 2. Rate constants k_3 and k_{-3} were estimated for each linear plot, and the corresponding average K_3 value is presented in Table 2.

The buffer dependence of k_3 was investigated with experimental set AP-9 (Table 1). Parallel to the finding for eq 1, HPO_4^{2-} was the only base found to affect the kinetics of eq 2 under the range of experimental conditions investigated. The buffer dependence of k_3 is depicted in Figure 4. The slope and intercept of this plot were used to estimate the corresponding k_3^0 and $k_3^{HPO_4}$ values (Table 2) with an expression of the form of eq 23. The reverse rate constants, k_{-3}^0 and $k_{-3}^{HPO_4}$, can be calculated by dividing the corresponding forward rate constants by K_3.

The molar absorptivity for N-chlorodimethanolamine at 242 nm (Table 3) was estimated using A_e and K_3 (Table 2) values and the N-chloroaminomethanol molar absorptivity (Table 3).

The kinetic and equilibrium constants presented in Table 2 were applied to predict complete stopped-flow photometry traces at relatively high $[CH_2O]_{T,0}$. A kinetic model including rate expressions for the five species involved in eqs 1, 2, and

8 was solved by a finite difference approach. As illustrated in Figure 5, the model represented the experimental data adequately.

Decomposition of *N*-Chloroaminomethanol and *N*-Chlorodimethanolamine. The formaldehyde addition reactions (eqs 1 and 2) practically reached equilibrium prior to a relatively slower decrease in absorbance resulting from the decompositions of *N*-chloroaminomethanol and *N*-chlorodimethanolamine. Four of the species involved in eqs 3−7 absorb light at 250 nm: monochloramine, *N*-chloroaminomethanol, *N*-chlorodimethanolamine, and *N*-chloromethanimine. It is subsequently demonstrated that, with the exception of tests performed at $p[H^+] < 5.5$, the rates of eqs 3 and 4 were much slower than that of eq 5. Accordingly, the overall decay rate for *N*-chloro species could be expressed as

$$-\frac{dC_{T,NCl}}{dt} = k_4[CH_2(OH)NHCl] + k_5[\{CH_2(OH)\}_2NCl] \quad (26)$$

with

$$C_{T,NCl} = [NH_2Cl] + [CH_2(OH)NHCl] + [\{CH_2(OH)\}_2NCl] \quad (27)$$

Equation 26 is valid only if the reaction of cyanide ion with monochloramine (eq 7) is much slower than eqs 3 and 4. The validity of this assumption is addressed in a later section.

The concentration of each *N*-chloro species can be expressed as a fraction of $C_{T,NCl}$ by combining the equilibrium expressions for eqs 1 and 2 with eq 27:

$$\frac{[NH_2Cl]}{C_{T,NCl}} = \alpha_0 =$$
$$\frac{1}{1 + K_1K_2[CH_2(OH)_2] + K_1^{\,2}K_2K_3[CH_2(OH)_2]^2} \quad (28)$$

$$\frac{[CH_2(OH)NHCl]}{C_{T,NCl}} = \alpha_1 =$$
$$\frac{K_1K_2[CH_2(OH)_2]}{1 + K_1K_2[CH_2(OH)_2] + K_1^{\,2}K_2K_3[CH_2(OH)_2]^2} \quad (29)$$

$$\frac{[\{CH_2(OH)\}_2NCl]}{C_{T,NCl}} = \alpha_2 =$$
$$\frac{K_1^{\,2}K_2K_3[CH_2(OH)_2]^2}{1 + K_1K_2[CH_2(OH)_2] + K_1^{\,2}K_2K_3[CH_2(OH)_2]^2} \quad (30)$$

Substitution of eqs 29 and 30 into eq 26 results in the following rate expression:

$$-\frac{dC_{T,NCl}}{dt} = \alpha_1(k_4 + k_5K_3K_1[CH_2(OH)_2])C_{T,NCl} \quad (31)$$

The total absorbance of the solution can be expressed as a function of $C_{T,NCl}$:

$$A = (\alpha_0\epsilon_0 + \alpha_1\epsilon_1 + \alpha_2\epsilon_2)C_{T,NCl} \quad (32)$$

ϵ_0, ϵ_1, and ϵ_2 are the molar absorptivities of monochloramine, *N*-chloroaminomethanol, and *N*-chlorodimethanolamine at 250 nm. Molar absorptivities (Table 3) were estimated by fitting the initial absorbance of all traces performed with phosphate buffer at $p[H^+] > 5.5$ with eq 32.
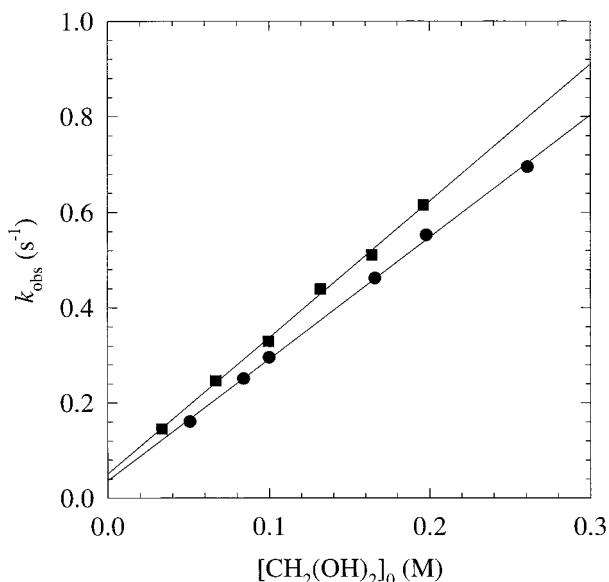
FIGURE 6. Observed and predicted apparent first-order rate constants corresponding to two experimental sets performed at relatively high $[CH_2O]_{T,0}$ and different buffer concentrations. Experimental conditions: (●) $[CH_2O]_{T,0} = 51.2-273$ mM, $p[H^+] = 6.89 \pm 0.06$, $[PO_4]_T = 0.012$ M, $[NH_2Cl]_0 = 0.472$ mM; (■) $[CH_2O]_{T,0} = 33.8-203$ mM, $p[H^+] = 6.91 \pm 0.02$, $[PO_4]_T = 0.018$ M, $[NH_2Cl]_0 = 0.495$ mM; 25.0 ± 0.1 °C, and $\mu = 0.1$ M (NaClO$_4$) for both sets (sets AP-7 and AP-8, Table 1).

The initial decay rates for traces corresponding to most experimental sets were first order:

$$-\frac{dA}{dt} = k_{obs}A \quad (33)$$

where A is absorbance and k_{obs} is the observed first-order rate constant.

Substitution of eq 32 into eq 33 gives an expression of the form of eq 31 with

$$k_{obs} = \alpha_1(k_4 + k_5K_3K_1[CH_2(OH)_2]) \quad (34)$$

Values for equilibrium constants K_1, K_2, and K_3 (Table 2) can be applied to calculate the fractions of *N*-chloro compounds for the range of experimental conditions investigated with phosphate buffer. The estimated fractions ranged from $\alpha_0 = 0.033$, $\alpha_1 = 0.369$, and $\alpha_2 = 0.597$ at $[CH_2O]_{T,0} = 0.0270$ M to $\alpha_0 = 0.003$, $\alpha_1 = 0.143$, and $\alpha_2 = 0.854$ at $[CH_2O]_{T,0} = 0.101$ M.

Rate Constants. Absorbance traces obtained for set DC-1 (Table 1) are shown in Figure 7. First-order reactions (eq 33) were observed in all four tests. Similarly, the initial decay rates for traces corresponding to most other experimental sets were also first order. A tendency of the apparent rate to deviate from initial first order, which was more pronounced near neutral $p[H^+]$, and $3.5 \leq p[H^+] \leq 5.5$ will be addressed subsequently. k_{obs} values were estimated from the initial slope of absorbance traces for all experiments performed at $[NH_2Cl]_0 = 0.5$ mM, $[CH_2O]_{T,0} = 47.3$ mM, and buffer concentration of 20 mM (phosphate, borate, or carbonate). Initial apparent first-order decay rates obtained at $2.8 < p[H^+] < 3.5$ and $5.5 < p[H^+] < 10.2$ are plotted against the corresponding $p[H^+]$ in Figure 8. As discussed previously, the rate of absorbance decay had a tendency to deviate from first order as reactions proceeded. The main reason for this deviation at $p[H^+] > 5$ was that the rate of monochloramine decomposition according to eq 7 became comparable to those for eqs 1−4 as the concentration of cyanide resulting from eqs 5 and 6 increased with time. The initial reaction time
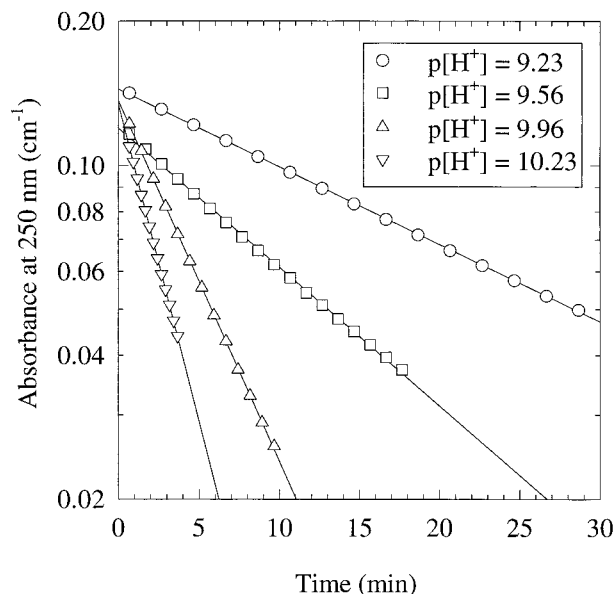
FIGURE 7. Experimental traces observed at $[NH_2Cl]_0 = 0.5$ mM, $[CH_2O]_{T,0} = 47$ mM, $p[H^+] = 9.2-10.2$, carbonate buffer concentration of 0.02 M, 25.0 ± 0.1 °C, and $\mu = 0.1$ M (NaClO$_4$) (set DC-1, Table 1).
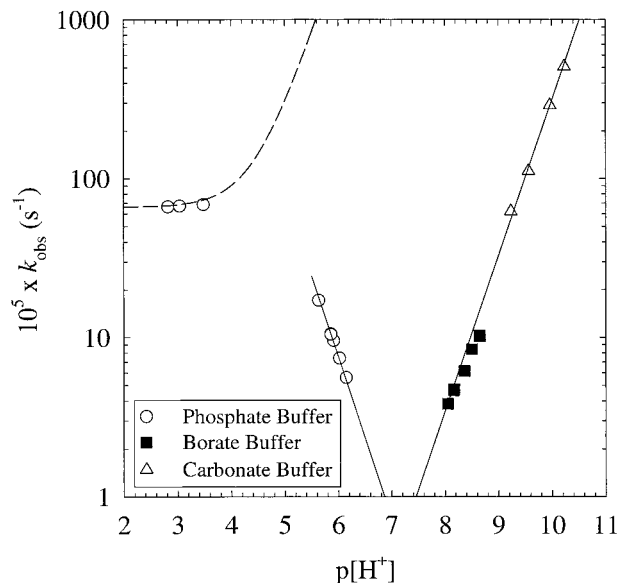
FIGURE 8. Effect of pH on the initial apparent first-order rate constant for tests performed at $[NH_2Cl]_0 = 0.5$, $[CH_2O]_{T,0} = 47.3$ mM, total buffer concentration of 20 mM, 25.0 ± 0.1 °C and $\mu = 0.1$ M (NaClO$_4$). Continuous regression lines correspond to the phosphate data at $p[H^+] = 5.5-6.5$ and carbonate data at $p[H^+] = 9.2-10.2$. Dashed line is a representation of k_6 based on k_6^0 and k_6^{OH} values in Table 2.

range for which the rate remained nearly first order was estimated for each trace by setting the criteria that the rate of eq 7 be generally less than 5% of the overall apparent rate. A trial-and-error approach was followed for this purpose using the rate constants reported by Schurter et al. (16) for eq 7.

Inspection of Figure 8 reveals the occurrence of both acid and base catalysis for $p[H^+] > 5.5$. k_{obs} reached an apparent constant value at $p[H^+] \approx 3$ due to a shift in limiting reactant from N-chloroaminomethanol and N-chlorodimethanol-amine to N-chloromethanimine as discussed in a subsequent section. First-order kinetics were not observed at $3.5 < p[H^+] < 5.5$.

$5.5 < p[H^+] < 6.5$. According to eq 34, a plot of k_{obs}/α_1 values against $[CH_2(OH)_2] \approx [CH_2(OH)_2]_0$ should be linear
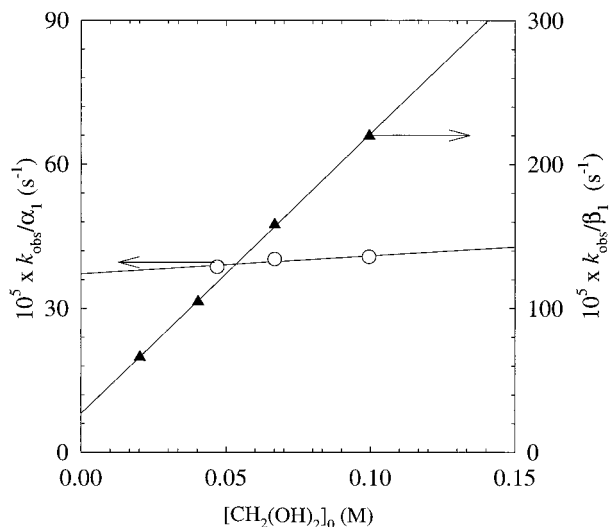
FIGURE 9. Effect of methanediol concentration on the initial apparent first-order rate constant for tests performed at (○) $[CH_2O]_{T,0} = 47-100$ mM, total phosphate buffer concentration of 20 mM, $p[H^+] = 5.8$, (NaClO$_4$) (set DP-4, Table 1), and (▲) $[CH_2O]_{T,0} = 20-100$ mM, total borate buffer concentration of 20 mM, $p[H^+] = 9.05$ (set DB-3, Table 1).

SCHEME 1
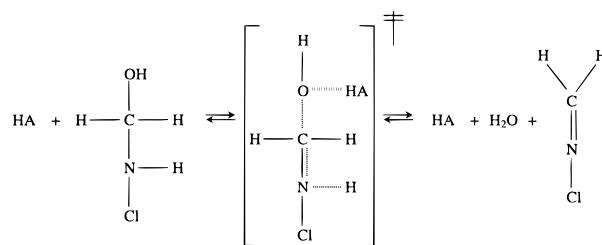
with slope $k_5K_3K_1$ and intercept k_4. As depicted in Figure 9 for set DP-4 data (Table 1), eq 3 was responsible for most of the decomposition of N-chloro species at $p[H^+] = 5.8$. On the basis of the criteria defined previously for interference by eq 7, first-order rate constants could only be determined for tests at high formaldehyde concentrations within this set. The results are consistent with acid-catalyzed dehydration of N-chloroaminomethanol to N-chloromethanimine. As shown in Scheme 1, the hydroxyl group of N-chloroamino-methanol is susceptible to protonation. Acid-catalyzed dehydration of N-chlorodimethanolamine would not be expected because the nitrogen atom has no proton to lose. Also, Antelo and co-workers performed a study on the decomposition rate of a similar compound, N-chlorodieth-anolamine, and found that base catalysis and not acid catalysis was the predominant decay pathway (37). Conse-quently, eq 33 simplifies to $k_{obs} = \alpha_1 k_4$ for traces run at $5.5 < p[H^+] < 6.5$.

Two acids, $H_2PO_4^-$ and H_3O^+, were checked for contribu-tion to k_4 within this $p[H^+]$ range. Analysis of the data for experimental set DP-5 (Table 1) revealed that the effect of $H_2PO_4^-$ was negligible. Consequently, the overall rate con-stant k_4 can be expressed as

$$k_4 = k_4^{H}[H^+] \qquad (35)$$

Values of k_{obs} obtained from trace data from sets DP-2-5 that met the criteria of lack of interference by eq 7 were used to determine the contribution of H^+ to the overall acid catalysis of eq 3. Resulting k_{obs}/α_1 values are plotted against $[H^+]$ in Figure 10. The rate constant k_4^H (Table 2) was estimated from the slope of the regression line in Figure 10.

8 < p[H⁺] < 9. The decomposition of N-chloro compounds in this p[H⁺] range was investigated with borate-buffered solutions (Table 1). In general, experimental k_{obs} values tended to be lower than expected. This deviation was more pronounced at relatively high values of buffer concentration, p[H⁺], and $[CH_2O]_{T,0}$. Boric acid, known to form cyclic borate esters with 1,2-diols (38), probably reacted with N-chloro-dimethanolamine. The following reaction is proposed to account for this effect:

$$B(OH)_3 + \{CH_2(OH)\}_2NCl \underset{}{\overset{K_B}{\rightleftharpoons}}$$
$$ClN\{CH_2O\}_2B(OH)_2^{-} + H_2O + H^+ \quad (36)$$
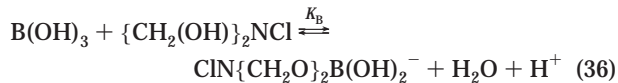
with K_B as the reaction equilibrium constant. The total concentration of N-chloro compounds is

$$C_{T,NCl} = [NH_2Cl] + [CH_2(OH)NHCl] + [\{CH_2(OH)\}_2NCl] + [ClN\{CH_2O\}_2B(OH)_2^{-}] \quad (37)$$

and the reaction rate expression is

$$-\frac{dC_{T,NCl}}{dt} = \beta_1(k_4 + k_5K_3K_1[CH_2(OH)_2])C_{T,NCl} = k_{obs}C_{T,NCl} \quad (38)$$

with β_1 substituting α_1 (see eq 34) as the new fraction for N-chloroaminomethanol:

$$\beta_1 = K_1K_2[CH_2(OH)_2]/\{1 + K_1K_2[CH_2(OH)_2] + K_1^2K_2K_3[CH_2(OH)_2]^2(1 + K_B[B(OH)_3]/[H]^+)\} \quad (39)$$

Equationss 38 and 39 are based on the assumptions that eq 36 is reversible and in rapid equilibrium with respect to eqs 3 and 4. Also, notice that according to eq 39, β_1 would decrease with increasing values of both p[H⁺] and $[CH_2O]_{T,0}$. This effect would be consistent with the observed trend in experimental k_{obs} values as a function of both p[H⁺] (Figure 8) and $[CH_2O]_{T,0}$.

Experimental k_{obs} values for data from sets DB-1−8 (Table 1) were fitted with eqs 38 and 39. For this purpose, k_4 and k_5 were assumed to include the following components:

$$k_4 = k_4^H[H^+] + k_4^{OH}[OH^-] \quad (40)$$

$$k_5 = k_5^{OH}[OH^-] \quad (41)$$

with k_4^H being the value determined previously (Table 2). Equations 40 and 41 were based on the assumption that the borate/boric acid buffer had a negligible catalytic effect on k_{obs} over the range of experimental conditions tested. Estimated fitting parameters K_B, k_4^{OH}, and k_5^{OH} are presented in Table 2. The dissociation constant used for boric acid was $pK_a = 8.97$ at 25 °C and $\mu = 0.1$ M (31). On the basis of $K_B = 1.42 \times 10^{-7}$, the fraction of total N-chloro compounds occurring as the proposed cyclic borate ester are estimated to range from 18% at p[H⁺] = 8.17 and $[CH_2O]_{T,0}$ = 0.0270 M to 55% at p[H⁺] = 9.05 and $[CH_2O]_{T,0}$ = 0.101 M.

Results for experimental set DB-3 (Table 1) are plotted in Figure 9 according to eq 38. The increase in both slope and intercept of the linear regressions with increasing p[H⁺] confirmed that both k_4 and k_5 included base catalysis components in accordance with eqs 40 and 41. N-Chloroaminomethanol and N-chlorodimethanolamine are both expected to undergo base catalysis since proton removal should occur in each case (Schemes 2 and 3).

The total absorbance of the solution can be expressed as a function of $C_{T,NCl}$:

$$A = (\beta_0\epsilon_0 + \beta_1\epsilon_1 + \beta_2\epsilon_2 + \beta_3\epsilon_3)C_{T,NCl} \quad (42)$$
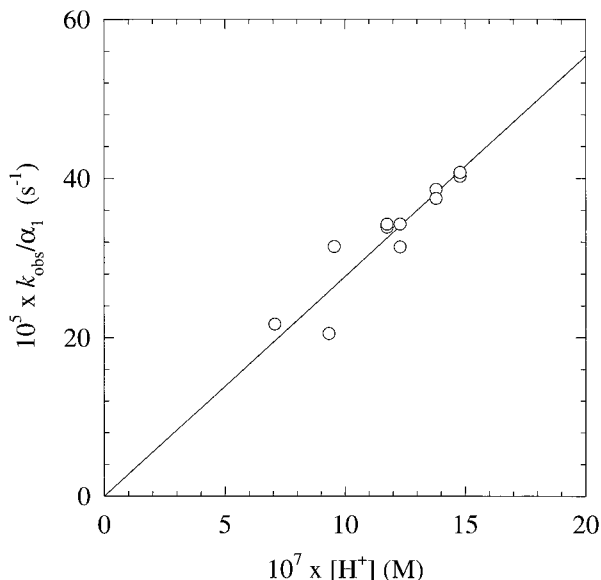
FIGURE 10. Effect of H⁺ concentration on the initial apparent first-order rate constant for tests performed at $[NH_2Cl]_0$ = 0.5 mM, $[CH_2O]_{T,0}$ = 47 mM, p[H⁺] = 5.8−6.2, total phosphate buffer concentration of 20 mM, 25.0 ± 0.1 °C, and μ = 0.1 M (NaClO₄) (sets DP-2−5, Table 1).

SCHEME 2
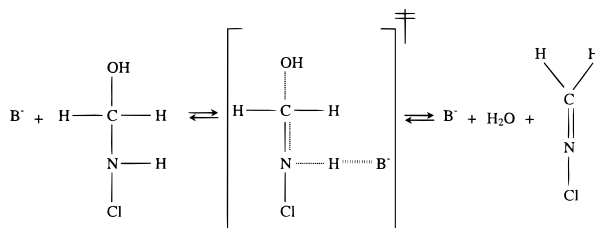
SCHEME 3
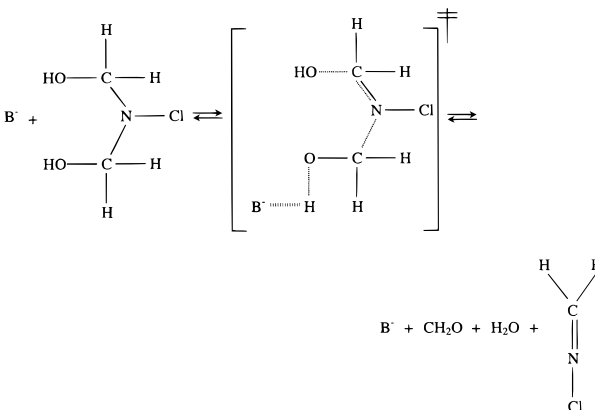
in which β_0, β_1, β_2, and β_3 are the molar fractions of monochloramine, N-chloroaminomethanol, N-chlorodimethanolamine, and cyclic borate ester; ϵ_0, ϵ_1, ϵ_2, and ϵ_3 are the corresponding molar absorptivities at 250 nm. The molar absorptivity of the cyclic borate ester (Table 3) was estimated by fitting the initial absorbance of all traces performed with borate buffer with eq 42 using the ϵ_0, ϵ_1, and ϵ_2 values previously determined for phosphate buffer solutions (Table 3).

p[H⁺] > 9 and p[H⁺] = 7.4. The validity of k_4^{OH} and k_5^{OH} values estimated with borate buffer data (Table 2) was checked by comparing to experimental results obtained for set DC-1 with carbonate buffer and for set DP-7 with
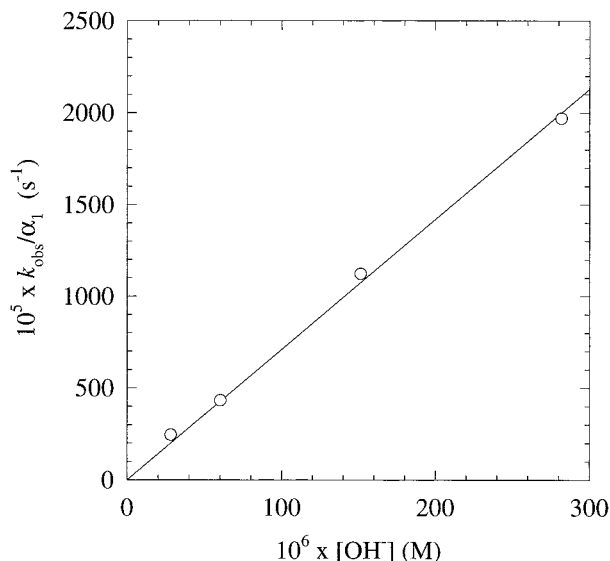
FIGURE 11. Comparison of experimental and predicted initial apparent first-order rate constants for tests performed at $[NH_2Cl]_0 = 0.5$ mM, $[CH_2O]_{T,0} = 47$ mM, $p[H^+] = 9.2-10.2$, carbonate buffer concentration of 0.02 M, 25.0 ± 0.1 °C, and $\mu = 0.1$ M (NaClO$_4$) (set DC-1, Table 1). Solid line corresponds to predicted values and is not a regression.
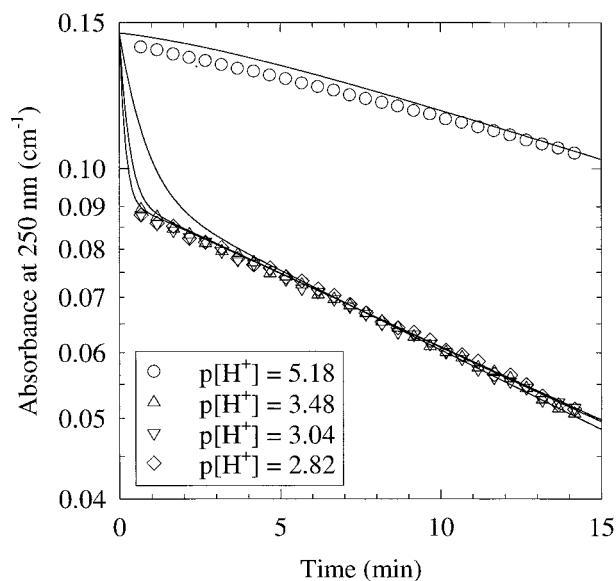
FIGURE 12. Comparison of experimental and predicted absorbance traces at $[NH_2Cl]_0 = 0.5$ mM, $[CH_2O]_{T,0} = 47$ mM, $p[H^+] = 2.8-5.2$, phosphate buffer concentration of 0.02 M, 25.0 ± 0.1 °C, and $\mu = 0.1$ M (NaClO$_4$) (set DP-1, Table 1).

phosphate buffer (Table 1). The comparison for set DC-1 is depicted in Figure 11. Very good agreement was found between predicted and experimental values. It should be noted that the line presented in the figure is not a regression of the data but rather that predicted with eqs 34, 40, and 41 using the k_4^{OH} and k_5^{OH} values in Table 2.

The apparent rate constant estimated with eqs 34, 40, and 41 using k_4^H, k_4^{OH}, and k_5^{OH} values in Table 2 for the conditions of experimental set DP-7, $k_{obs} = 1.08 \times 10^{-5}$ s^{-1}, was within 10% of the average initial rate constant value $k_{obs} = 0.99 \times 10^{-5}$ s^{-1} obtained for the experimental traces. These results also confirmed the assumptions made in eqs 40 and 41 that water-assisted rate terms were negligible as compared to the acid and base catalysis terms.

$p[H^+] < 5.5$. Experimental results observed for set DP-1 (Table 1) were consistent with a shift in rate-limiting reaction.

The decomposition of N-chloromethanimine (eq 5) is proposed as the rate-limiting reaction at $p[H^+] < 3$. The presence of N-chloromethanimine was supported by a shift in the spectrum of the reaction solutions at this pH range. The analysis of experimental traces at $3.0 < p[H^+] < 5.5$ required taking into consideration the simultaneous decomposition of N-chloroaminomethane and N-chlorodimethanolamine (eqs 3 and 4) and the formation and decomposition of N-chloromethanimine (eq 5) or

$$\frac{d[CH_2NCl]}{dt} = \alpha_1 k_4(C_{T,NCl} - [CH_2NCl]) - k_6[CH_2NCl] \quad (43)$$

$$-\frac{dC_{T,NCl}}{dt} = k_6[CH_2NCl] \quad (44)$$

where k_6 is the rate constant for N-chloromethanimine decomposition, α_1 and k_4 are defined by eqs 29 and 40, and the total concentration of N-chloro compounds is given by

$$C_{T,NCl} = [NH_2Cl] + [CH_2(OH)NHCl] + \\ [\{CH_2(OH)\}_2NCl] + [CH_2NCl] \quad (45)$$

Integration of eqs 43 and 44 resulted in the following analytical solutions:

$$C_{T,NCl} = a_1 e^{\lambda_1 t} + a_2 e^{\lambda_2 t} \quad (46)$$

$$[CH_2NCl] = -\frac{1}{k_6}(a_1\lambda_1 e^{\lambda_1 t} + a_2\lambda_2 e^{\lambda_2 t}) \quad (47)$$

with

$$a_1 = \frac{\lambda_2}{\lambda_2 - \lambda_1} C_{T,NCl,o} \quad (48)$$

$$a_2 = \frac{\lambda_1}{\lambda_1 - \lambda_2} C_{T,NCl,o} \quad (49)$$

$$\lambda_1,\lambda_2 = \frac{-(\alpha_1 k_4 + k_6) \pm \sqrt{(\alpha_1 k_4 + k_6)^2 - 4\alpha_1 k_4 k_6}}{2} \quad (50)$$

Finally, total solution absorbance can be expressed as a function of $C_{T,NCl}$ and $[CH_2NCl]$:

$$A = (\alpha_0\epsilon_0 + \alpha_1\epsilon_1 + \alpha_2\epsilon_2)(C_{T,NCl} - [CH_2NCl]) + \\ \epsilon_4[CH_2NCl] \quad (51)$$

where ϵ_0, ϵ_1, ϵ_2, and ϵ_4 are the molar absorptivities of monochloramine, N-chloroaminomethanol, N-chlorodimethanolamine, and N-chloromethanimine at 250 nm. The molar absorptivity for N-chloromethanimine, estimated by fitting the initial absorbance of the trace performed with phosphate buffer at $p[H^+] = 2.8$ (set DP-1) with eq 51, is also presented in Table 3.

Equations 46–51, with the k_4^H value from Table 2, were used to fit traces for experimental set DP-1. A trial and error analysis revealed that eq 5 was base-catalyzed according to

$$k_6 = k_6^0 + k_6^{OH}[OH^-] \quad (52)$$

where k_6^0 and k_6^{OH} are the rate constants for water and hydroxide ion catalysis. Values of k_6^0 and k_6^{OH}, calculated from fitting of the experimental traces, are presented in Table 2.

Good agreement was found between fitted curves and experimental traces as depicted in Figure 12. The deviation observed at initial reaction times might have resulted from

SCHEME 4
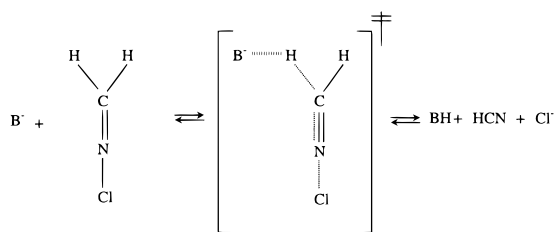
neglecting the contribution by eq 7 to the overall rate of *N*-chloro compounds decomposition.

The proposed mechanism for base-catalyzed decomposition of *N*-chloromethanimine is depicted in Scheme 4. Proton removal is required for the formation of HCN. The rates of water and hydroxide assisted decay pathways are significantly higher for *N*-chloromethanimine than those for the decay of *N*-chloroaminomethanol and *N*-chlorodimethanolamine (see Figure 8). Consequently, *N*-chloromethanimine should not accumulate to significant levels at p[H$^+$] > 5.5.

Acknowledgments

Literature Cited

(1) Krasner, S. W.; McGuire, M. J.; Jacangelo, J. G.; Patania, N. L.; Reagan, K. M.; Aieta, E. M. *J. Am. Water Works Assoc.* **1989**, *80*, 41−53.

(2) U.S. EPA. *Fed. Regist.* **1996**, *61*, 24353−24388.

(3) World Health Organization. *Guidelines for Drinking Water Quality*, 2nd ed.; World Health Organization: Geneva, 1993; Vol. I.

(4) Pedersen, E. J., III; Mariñas, B. J. *Proceedings of the 1995 American Water Works Association Annual Conference, Water Research,* Anaheim, CA, June 18−22, 1995; American Water Works Association: Denver, 1995; pp 359−369.

(5) Pedersen, E. J., III; Urbansky, E. T.; Mariñas, B. J.; Margerum, D. W. *Preprints of Papers Presented at the 210th American Chemical Society National Meeting, Division of Environmental Chemistry,* Chicago, IL, August 20−24, 1995; American Chemical Society: Washington, DC, 1995; Vol. 35, No. 2, pp 710−713.

(6) Weinberg, H. S.; Glaze, W. H.; Krasner, S. W.; Sclimenti, M. J. *J. Am. Water Works Assoc.* **1993**, *85*, 72−85.

(7) Glaze, W. H.; Koga, M.; Cancilla, D. *Environ. Sci. Technol.* **1989**, *23*, 838−847.

(8) Richardson. In *Encyclopedia of Environmental Analysis and Remediation*; Meyers, R., Ed.; Wiley: New York, 1998; p 1398.

(9) Hand, V. C.; Snyder, M. P.; Margerum, D. W. *J. Am. Chem. Soc.* **1983**, *105*, 4022−4025.

(10) Cocivera, M.; Fyfe, C. A.; Effio, A.; Vaish, S. P.; Chen, H. E. *J. Am. Chem. Soc.* **1976**, *98*, 1573−1578.

(11) Jencks, W. P. In *Physical Organic Chemistry*, Vol. 2; Cohen, S. G., Streitwieser, A., Jr., Taft, R. W., Eds.; Interscience: New York, 1964; pp 63−122.

(12) Lowry, T. H.; Richardson, K. S. *Mechanism and Theory in Organic Chemistry*, 3rd ed.; Harper & Row: New York, 1987; pp 661−709.

(13) March, J. *Advanced Organic Chemistry*, 4th ed.; Wiley: New York, 1992; pp 796−800.

(14) Sollenberger, P. Y.; Martin, R. B. In *The Chemistry of the Amino Group*; Patai, S., Ed.; Interscience: New York, 1968; pp 367−380.

(15) Wade, L. G., Jr. *Organic Chemistry*; Prentice Hall: Englewood Cliffs, NJ, 1987; pp 804−806.

(16) Schurter, L. M.; Bachelor, P. P.; Margerum, D. W. *Environ. Sci. Technol.* **1995**, *29*, 1127−1134.

(17) Ohya, T.; Kanno, S. *Chemosphere* **1989**, *19*, 1835−1842

(18) Hirose, Y.; Maeda, N.; Ohya, T.; Nojima, K.; Kanno, S. *Chemosphere* **1988**, *17*, 865−873.

(19) Maeda, N.; Ohya, T.; Nojima, K.; Kanno, S. *Chemosphere* **1987**, *16*, 2249−2258.

(20) Hirose, Y.; Maeda, N.; Ohya, T.; Nojima, K.; Kanno, S. *Chemosphere* **1989**, *18*, 2101−2108.

(21) Sawicki, E.; Sawicki, C. R. *Aldehydes−Photometric Analysis*; Academic: New York, 1975; p 210.

(22) Hasse, H.; Maurer, G. *Ind. Eng. Chem. Res.* **1991**, *30*, 2195−2200.

(23) Hahnenstein, I.; Albert, M.; Hasse, H.; Kreiter, C. G.; Maurer, G. *Ind. Eng. Chem. Res.* **1995**, *34*, 440−450.

(24) Walker, J. F. *Formaldehyde*, 3rd ed.; Reinhold: New York, 1964; pp 54−107.

(25) Gray, E. T., Jr.; Margerum, D. W.; Huffman, R. P. In *Organometals and Organometalloids, Occurrence and Fate in the Environment*; Brinckman, F. E., Bellama, J. M., Eds.; ACS Symposium Series 82; American Chemical Society: Washington, DC, 1978; pp 264−277.

(26) Kumar, K.; Day, R. A.; Margerum, D. W. *Inorg. Chem.* **1986**, *25*, 4344−4350.

(27) Kawasaki, A.; Ogata, Y. *Mem. Fac. Eng., Nagoya Univ.* **1967**, *19*, 1−45.

(28) Cross, C. F.; Bevan, E. J.; Bacon, W. *J. Chem. Soc. Trans.* **1910**, *97*, 2404−2406.

(29) Lindsay, M.; Soper, F. G. *Proc. Chem. Soc., London* **1946**, 791−792.

(30) Le Cloirec, C.; Martin, G. *Water Chlorination*; Jolley, R. L., Bull, R. J., Davis, W. P., Katz, S., Roberts, M. H., Jr., Jacobs, V. A., Eds.; Lewis Publishers: Chelsea, MI, 1985; pp 821−834.

(31) Smith, R. M.; Martell, A. E. *Critical Stability Constants. Volume 4: Inorganic Complexes*; Plenum Press: New York, 1976.

(32) Bell, R. P.; Evans, P. G. *Proc. R. Soc., Ser. A* **1966**, *291*, 297−323.

(33) Los, J. M.; Roeleveld, L. F.; Wetsema, B. J. C. *J. Electroanal. Chem.* **1977**, *75*, 819−837.

(34) Skell, P.; Suhr, H. *Chem. Ber.* **1961**, *94*, 3317−3327.

(35) Ferriol, M.; Gazet, J.; Rizk-Ouaini R. *Anal. Chim. Acta* **1990**, *231*, 161−163.

(36) Bernasconi, C. F. *Relaxation Kinetics*; Academic: New York, 1976; pp 3−10, 20−31.

(37) Antelo, J. M.; Arce, F.; Casal, D.; Rodriguez, P.; Varela, A. *Tetrahedron* **1989**, *45* (12), 3955−3966.

(38) Shriver, D. F.; Atkins, P. W.; Langford, C. H. *Inorganic Chemistry*; W. H. Freeman and Company: New York, 1990; p 336.